

Preliminary investigations of compatible nanolime treatments on Indiana limestone and weathered marble stone

OTERO, Jorge, CHAROLA, Elena and STARINIERI, Vincenzo
<<http://orcid.org/0000-0002-7556-0702>>

Available from Sheffield Hallam University Research Archive (SHURA) at:
<http://shura.shu.ac.uk/26509/>

This document is the author deposited version. You are advised to consult the publisher's version if you wish to cite from it.

Published version

OTERO, Jorge, CHAROLA, Elena and STARINIERI, Vincenzo (2020). Preliminary investigations of compatible nanolime treatments on Indiana limestone and weathered marble stone. *International Journal of Architectural Heritage*.

Copyright and re-use policy

See <http://shura.shu.ac.uk/information.html>

26 **1. Introduction**

27 In conservation work, there is a dictum that consolidation should be done using materials which are compatible
28 with the original substrate [1]. This statement from the Venice Charter for the Restoration of Historic Monuments,
29 sums up the importance of the compatibility of any treatments applied to Cultural Heritage structures with
30 significant value (artistic, cultural or historical). Calcareous stones are important construction materials employed
31 in Cultural Heritage and widely used around the world. These historic structures are susceptible to several
32 weathering processes, which cause structures to lose some of their original properties [2].

33
34 The mechanical properties of weathered historic structures are aimed to be restored using consolidating products.
35 One of the most important points is that the used consolidant must meet the “compatibility with the original
36 substrate” condition, as stated by the 1972 Italian Carta del Restauro [3] and considered as one of the three
37 conservation principles by Brandi [4]. In the last four decades, most of the consolidating products used for
38 restoration treatments are silica-based precursors (e.g. TEOS or MTMOS) [5]. These products were originally
39 developed for the consolidation of sandstone, and then extended to other types of stone thanks to their ease of
40 application, good penetration capability, immediate strength enhancement and effectiveness for silica-based
41 substrates [6]. However, in the case of calcareous substrates, these consolidants present low physical and
42 mechanical compatibility with the treated material, which in many cases cause cracks and significant damage in the
43 long term [5-7]. For this reason, lime-based consolidants such as lime-water were traditionally preferred due to
44 their higher compatibility with the matrix and durability [8,9]. The consolidation effect of lime-water (aqueous
45 suspension of lime particles) occurs by the carbonation reaction of lime particles (portlandite ($\text{Ca}(\text{OH})_2$)) when
46 exposed to atmospheric CO_2 and H_2O , producing new CaCO_3 , which is obviously totally compatible with the
47 matrix of calcareous materials. Thus, this method presents a high compatibility with the substrate as it “*adds more*
48 *of its natural cementing materials to the substrate*”. However, the lime-water consolidation technique presents
49 some important limitations such as a reduced impregnation depth (few millimetres), a very slow carbonation
50 process, a low amount of lime particles applied in each application, and a limited access of lime particles to the
51 pores with small diameters; which in many cases leads to unsatisfactory treatments [10].

52
53 Nanolime is based on the lime-water technique and keeps the same high compatibility with the substrate but
54 presents higher consolidation properties due to the smaller size of the lime nanoparticles and especially the higher

55 amount of consolidant and a lower amount of water introduced to the stones [8, 11, 12]. Nanolime has been
56 successfully synthesized by several methods: diols [13, 14], w/o microemulsions [15], aqueous solutions [16,17],
57 solvothermal reactions [18, 19] plasma metal reaction method [20] or anion exchange kinetics [21, 22]. The latter
58 method synthesized nanoparticles which present higher reactivity and smaller particle size [23, 24].

59

60 The consolidation effect of nanolime occurs by the same carbonation reaction as for lime-water; however, the
61 smaller size of the lime particles improves the penetration providing access to smaller pores and faster carbonation
62 process due to the higher specific surface of nanoparticles [12]. Since its development in 2001, nanolime has been
63 effectively tested for the consolidation of several substrates such as wall-paintings [13], lime-mortars [24],
64 limestones [25], biocalcarenes [23,26], and other historic materials such as paper [16], canvas [27], bones [28] or
65 wood [18]. Recently this type of nanolime has been also applied successfully on in-situ and long-term applications
66 [19, 29, 30, 31, 32].

67

68 **2. Research Aim**

69 This paper describes the preliminary investigations of compatible nanolime treatments for Indiana limestone, a
70 stone that has been used in many buildings in the US, as well as for weathered marble, to test out its effectiveness
71 prior to testing it in-situ on the weathered marble (from Texas, Md) sills of the west facade of the Reynolds Center,
72 previously the Patent Office Building, which houses both the Smithsonian's National Portrait Gallery and the
73 American Art Museum (Washington, D.C., USA). The consolidation effectiveness of two types of nanolime
74 (dispersed in ethanol and isopropanol) was assessed by studying changes in porosity, drilling resistance, superficial
75 cohesion and aesthetic appearance.

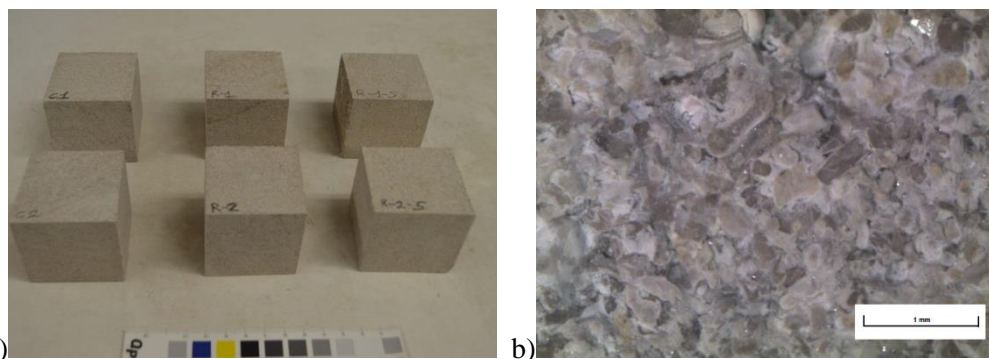
76

77 **3. Materials and methods**

78 *3.1 Limestone and Marble Samples*

79 – **Indiana limestone:** This stone, which is shown in Figure 1, is a limestone which is one of the most
80 commonly used building materials in the USA [33]. The stone is a sedimentary rock composed of bioclasts
81 and intraclasts cemented together by sparry calcite cement. The rock can be classified as a biointrasparite

82 [34] or Grainstone [35]. This stone was cut into 5 x 5 x 5 mm cubes for testing. This stone was referred to
83 as “I”.



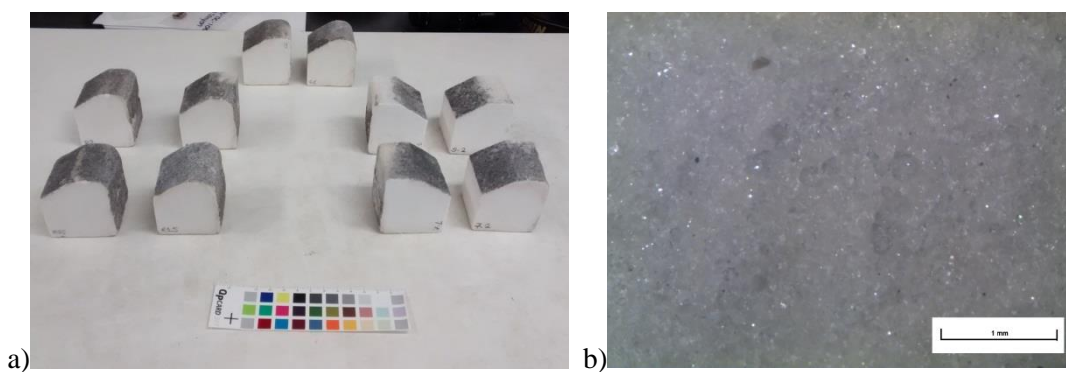
85 a) Indiana limestone cubic samples; b) stereomicroscope image of the limestone.
86 **Figure 1.** a) Indiana limestone cubic samples; b) stereomicroscope image of the limestone.

87
88 The elemental composition of this stone was calculated by XRF which shows that the stone is composed of
89 97.7 (± 0.2) of Ca, 0.81 (± 0.01) of Si, 0.45 (± 0.003) of P, 0.18 (± 0.001) of Fe, 0.61 (± 0.02) of Mg, 0.19
90 (± 0.001) of S and 0.03 (± 0.001) of Sr.

91
92 The mineralogical composition was determined by X-Ray Diffraction (PANalytical XPert PRO) where
93 XRD patterns were recorded with a step size of $0.026^\circ 2\theta$, in the angular range $20\text{-}70^\circ 2\theta$. The samples were
94 ground and sieved through an $80\ \mu\text{m}$ sieve mesh and placed over an XRD zero-background sample holder.
95 X-ray data were fitted using the pseudo-Voigt profile function. Specimen displacement, polynomial
96 coefficients for the background function, lattice parameters, profile parameters, and Gaussian and
97 Lorentzian profile coefficients were refined and XRD data was analysed by Rietveld refinements [36, 37].
98 XRD-Rietveld refinement shows that the only mineral detected is calcite (CaCO_3 , ICSD #00-005-0586),
99 suggesting that any other mineral phases (e.g. feldspar containing P, Si, Fe, Mg, Sr and S, which were
100 elements detected by the XRF) could be present in amorphous or poorly crystallised phases or in amounts
101 below the instrument detection level ($< 1\%$).

102
103 The pore structure was determined by Mercury Intrusion Porosimetry (MIP) which shows that the porosity
104 of this stone is 11.41 (± 0.86) % and its density is $1.974 (\pm 0.121)\ \text{g/cm}^3$

106 – **Weathered marble:** This stone, which is shown in Figure 2, is a weathered marble which was probably
 107 part of a cornice from a building to be remodelled, in Washington D.C, USA. It was taken from a pile of
 108 architectural marble blocks stored in the stone deposit at the Smithsonian Garber facility (Suitland, Md.).
 109 This stone presents similar weathering conditions to the weathered marble sills of the west facade of the
 110 Smithsonian’s National Portrait Gallery and the American Art Museum (Washington, D.C., USA). The
 111 stone is a fine-grained marble with two weathered surfaces (black crust). This cornice was cut into 50 x 50
 112 x 50 mm cubes with one of the faces being curved as shown in Figure 1a. This stone is referred to as “M”.



114 a) b)
 115 **Figure 2.** a) marble samples; b) stereomicroscope image of the marble sample

116
 117 The elemental composition of this stone was determined by XRF (Philips PW2400) on pressed powder
 118 samples (Retsch PP-40 pellet press). XRF results for the superficial black crust and the core of this stone
 119 are reported in Table 1.

120
 121 XRD-Rietveld refinement shows that the only detected mineral in the marble core is Calcite (CaCO_3 , ICSD
 122 #00-005-0586). However, quantitative analysis by Rietveld refinement of the black crust shows the
 123 mineralogical composition of the black crust is 84.4% calcite (CaCO_3 , ICSD #00-005-0586), ICSD#
 124 980086161) and 15.6% gypsum (calcium sulphate, CaSO_4 , ICSD# 01-076-1746). This result was
 125 confirmed by XRF (Table 2), which showed that the black crust consists mainly of gypsum (CaSO_4),
 126 probably resulting from the reaction of CaCO_3 with acidic rain [38].

127
Table 1. XRF analysis of the marble sample (wt %).

	Ca	P	Si	Al	S	Sr	Ti
Core	98.7	0.69	0.38	-	-	0.04	0.19

	(±0.3)	(±0.03)	(±0.1)		(±0.02)	(±0.002)
Black	96.4	0.41	0.45	0.14	2.4	
crust	(±0.3)	(±0.01)	(±0.06)	(±0.02)	(±0.03)	-

The pore structure of the weathered portion of the stone (outer 1 cm from the surface) was determined by Mercury Intrusion Porosimetry (MIP) by means of a PASCAL 140/240 instrument. The contact angle was taken to be 140°. Samples for MIP consisted of two stone fragments measuring approximately 8x8x15 mm which were dried in a fan-assisted oven at 60 °C until constant weight. MIP results shows that the porosity of the weathered surface is 6.0 (±0.52) % and the density is 2.144 (±0.08) g/cm³.

3.2 Nanolimes

Nanolime was synthesized through an anionic exchange process carried out at room conditions (± 50% RH, ± 20°C) by mixing under moderate stirring an anion exchange resin (Dowex Monosphere 550A OH by Dow Chemical) with an aqueous calcium chloride solution (CaCl₂ by Sigma-Aldrich), as described in the literature [21, 22, 39]. The concentration of chlorides was monitored during the process using a chloride strip (Fisherbrand® Chloride Strips). The decrease of chloride content during the synthesis was very rapid and the synthesis was stopped when the ion exchange process was completed (zero kinetic exchange), with a residual chloride content below 100 mg/L. Following the synthesis, the supernatant water of the produced nanolime was extracted through a pipette and substituted by an alcohol maintaining the concentration at 25 g/L. Two nanolime dispersions were prepared: i) 25 g/L nanoparticles in isopropanol (**IP25**); ii) 25 g/L nanoparticles in ethanol (**ET25**). The synthesized nanolime presents nanoparticles with size of approximately 20-80 nm, which are highly reactive to carbonation [11, 24, 25-27].

A small residual water (W = 5%) remained in the IP25 and ET25 dispersions, as this practice enhances the carbonation process [30]. Dispersions were kept in a refrigerator (T < 5 °C) prior to the application to minimize the Ca(OH)₂ particles conversion into Ca alkoxides [40].

3.3 Nanolime treatments

154 Samples were kept at laboratory conditions (50% (± 5) RH) for 7 days before treatment. The treatments were
155 carried out by brush in the same laboratory conditions. Treatments started two days after the nanolime synthesis to
156 increase their effectiveness [40]. Prior to the treatment, both nanolime dispersions (**ET25** and **IP25**) were placed in
157 an ultrasonic bath (60 Hz) for 30 minutes to minimize nanoparticle aggregation. Each nanolime was applied by
158 brush on a dry and clean surface of the specimens. IP25 was applied by brushing on two of the weathered faces of 8
159 marble specimens (**M**), whereas E25 was applied by brushing on 4 Indiana limestone samples (**I**). Previous
160 research showed that nanolime deposition in-depth within a substrate can be highly influenced by the nanolime
161 evaporation rate, being nanolime products with slightly slower evaporation rate more suitable for coarse porous
162 substrates and nanolime with faster evaporation rate more suitable for fine porous substrates [19]. Based on this
163 findings, nanolime dispersed in ethanol was applied to the marble samples due to the higher evaporation rate, while
164 nanolime in isopropanol, which is the most commonly used solvent for nanolime, was used for the Indiana
165 limestone samples.

166 The application was stopped when no absorption was observed (surface remains wet for at least one minute).
167 Following saturation, the samples were left to dry and then retreated again after 24 hours when samples were
168 completely dry. The treatment was repeated twice for both nanolimes. Upon treatment completion, the marble
169 samples (**M**) were stored in different environments to evaluate the influence of Relative Humidity on nanolime
170 carbonation: i) two of the treated marble samples were placed in a desiccator with a saturated solution of $\text{Mg}(\text{NO}_3)_2$
171 (RH~55%), which were referred to as **M55**; ii) two of the treated marble samples were placed in a desiccator with a
172 saturated solution of NaCl (RH~75%), which were referred to as **M75**; iii) two samples of treated marble were
173 exposed to the room environment conditions (50 \pm 5% RH, T = 20 \pm 5 $^\circ$ C), which were referred to as **MR**; and iv) two
174 of each treated marble were exposed to room conditions and daily sprayed with carbonated water at room
175 conditions, which were referred to as **MRS**. A set of 2 untreated marble control samples (**M-CO**) were stored in the
176 same room.

177 For the Indiana limestone, treated samples were kept in two environments: i) two of the treated Indiana samples
178 were exposed to the room environment conditions (50 \pm 5% RH, T = 20 \pm 5 $^\circ$ C), which were referred to as **IR**; and ii)
179 two other treated Indiana samples were exposed to room conditions and were sprayed daily with carbonated water
180 (~10 mL of commercial carbonated sparkling water containing approximately 6-8 g/L CO_2 was daily used) at room
181 conditions, which were referred to as **IRS**. A set of untreated control samples was also stored in the same room

182 environment conditions, **IR-CO** (control samples of Indiana). All samples were analysed after curing them for 28
183 days in the above conditions.

184

185 *3.4 Consolidation effectiveness*

186

187 For the Indiana samples (I), apparent porosity was measured, for each treatment, by immersing two cubic samples
188 in water for 48 hours at room atmosphere as described in ASTM C 67-00 [41]. For the marble samples (M), pore
189 size distribution and open porosity were measured by MIP. Tests were carried out on two samples taken from the
190 treated surfaces (the outer section up to a depth of 50 mm) and on two control samples. MIP was only carried out
191 on Marble samples due to the lack of availability of I samples.

192

193 The influence of nanolime treatments on both Indiana (I) and marble (M) surface cohesion was evaluated by
194 'Scotch Tape Test' (STT) according to ASTM, 2009 [42]. The test was carried out on treated and control samples
195 with a mean of 9 measures for each sample.

196

197 The consolidation action of both nanolimes was also evaluated by means of a Drilling Resistance Measurement
198 System (DRMS) from SINT-Technology, regularly used in the literature for assessing consolidation effectiveness
199 [43]. Tests were performed on both control and treated samples using drill bits of 5 mm diameter, rotation speed of
200 600 rpm, rate of penetration of 15 mm/min and penetration depth of 20 mm. Drilling resistance values were
201 calculated as the mean of 6 tests per each treatment.

202

203 The cross-section area of the surfaces of both Indiana and marble treated and control samples were observed under
204 a Scanning Electron Microscope (Hitachi S-3700N). Micro-graphs were taken with an ETD detector and an
205 accelerating voltage of 20 kV. Specimens were coated with a 20nm thick layer of gold using a Quorum Q150T
206 coater unit to prevent surface charging.

207

208 Any colour changes in both stones caused by treatments were evaluated with a spectrophotometer (Minolta
 209 CM508D Colorimeter) with the CIE-Lab system [44], using 30 readings taken in different areas per each treated
 210 and control sample. Total colour variation (ΔE) was calculated by the formula:

$$\Delta E = \sqrt{\Delta L^{*2} + \Delta a^{*2} + \Delta b^{*2}}$$

211 where ΔL^* is the change in luminosity (white-black parameter), Δa^* (red-green parameters) and Δb^* (blue-yellow
 212 parameters) where the difference is with respect to the treated and the control sample.

213

214

215 **4. Results and Discussions**

216 *4.1 Consolidation effectiveness*

217

218 The apparent porosity of cubic Indiana limestone samples treated with ET25 was obtained by immersing the
 219 samples for 24 hours in water at atmospheric pressure. Table 2 shows apparent porosity and open porosity of
 220 treated and untreated samples. Both treated samples, IR (stored in room condition) and IRS (stored in room
 221 condition and regularly sprayed with carbonated water), have slightly lower porosities than the control. This
 222 suggests that a certain amount of nanolime penetrated and carbonated in the Indiana limestones, although the high
 223 standard deviation makes this decrease not statistically significant.

Table 2. Calculated Apparent porosity (% g/g) and Open porosity (cm^3/cm^3)

Sample	I-CO	IR	IRS
Apparent Porosity % w/w	5.99 (± 0.52)	5.75 (± 0.44)	5.88 (± 0.39)
Open Porosity % v/v	13.44 (± 0.4)	12.96 (± 0.21)	13.04 (± 0.31)

224

225

226 The pore structure properties of the weathered marble treated with IP25 and control samples were obtained by MIP
 227 and are summarised in Table 3. It is evident that all treatments affected the pore structure of the weathered marble
 228 by reducing the open porosity. The highest porosity decrease was observed for the samples which have been treated
 229 and sprayed regularly with carbonated water, MRS (~60% decrease), followed by those treated and kept in a 75%
 230 RH environment, M75 (~50% decrease). This is in line with the literature, as is well-known that the carbonation
 231 process is strongly influenced by moisture and CO_2 exposure [2].

Table 3. Pore structure properties of treated and

control marble samples measured by MIP

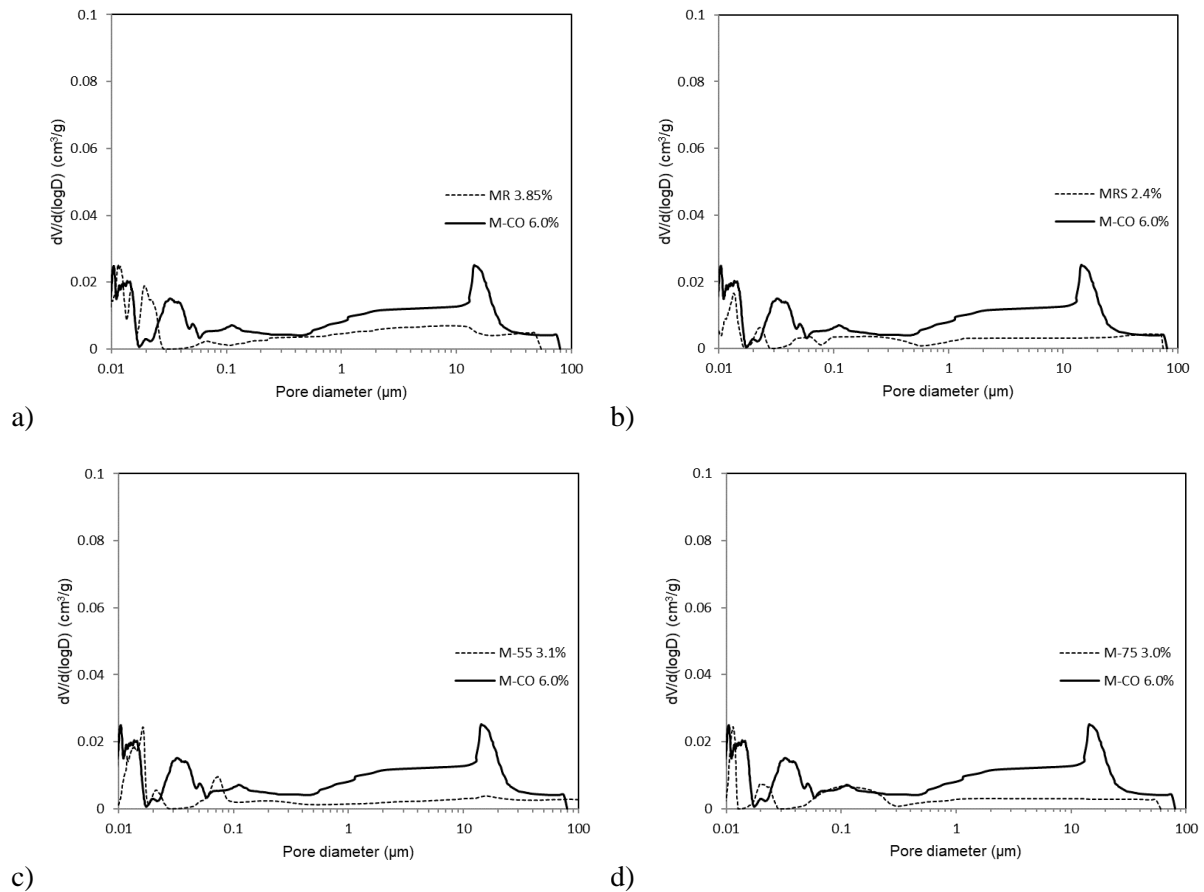
Sample	Open porosity (%)	Total pore surface area (m ² /g)
M-CO	6.00 (±0.24)	3.49 (±0.11)
MR	3.85 (±0.33)	2.35 (±0.19)
MRS	2.44 (±0.12)	1.48 (±0.12)
M55	3.11 (±0.29)	1.38 (±0.09)
M75	3.00 (±0.30)	1.76 (±0.18)

232

233

234 The pore size distributions of treated and untreated marble samples are shown in Figure 3. All treatments yielded a
 235 reduction in the population of pores with diameters between 0.02 μm and 30 μm, and this reduction is more
 236 pronounced for the samples treated with MRS, M-75 and M-55. The pore size regions of 0.1-0.2 μm and 30-50 μm
 237 seem to have been less affected by the treatments.

238



239

240 **Figure 3.** Differential volume of intruded mercury versus pore diameter of treated and untreated marble samples: a) MR; b)
 241 MRS; c) M55; d) M75.

242

243 The results of the Scotch Tape Test (STT) for both Indiana limestone and weathered marble are shown in Table 4.

244 All treatments yielded decreased values for the material removed ($\Delta W \approx 54 - 83\%$). These results confirm that all

245 surfaces are more compact after nanolime treatments in all tested environmental conditions. The samples sprayed
 246 with carbonated water (IRS and MRS) yielded the highest increase in superficial cohesion ($\Delta W \approx 77.2$ and 82.8% ,
 247 respectively). Marble samples stored at 75%RH (M75) yielded higher superficial cohesion than marble samples
 248 stored at 55%RH (M55), confirming that keeping samples in high relative humidity environments ($\sim 75\%$ RH)
 249 increases the consolidation effectiveness [45].

250

Table 4. Scotch Tape Test (STT): experimental results

	Released material (mg/cm²)	ΔW (%)	SD
ICO	5.59	-	0.86
IR	2.55	54.3	0.93
IRS	1.28	77.2	0.19
M-CO	9.01	-	2.17
MR	3.56	60.5	1.66
MRS	1.56	82.8	1.47
M55	4.52	49.9	1.78
M75	2.9	67.9	1.54

Scotch area: 3 x 1.5 cm; SD (standard deviation of released material)

251

252

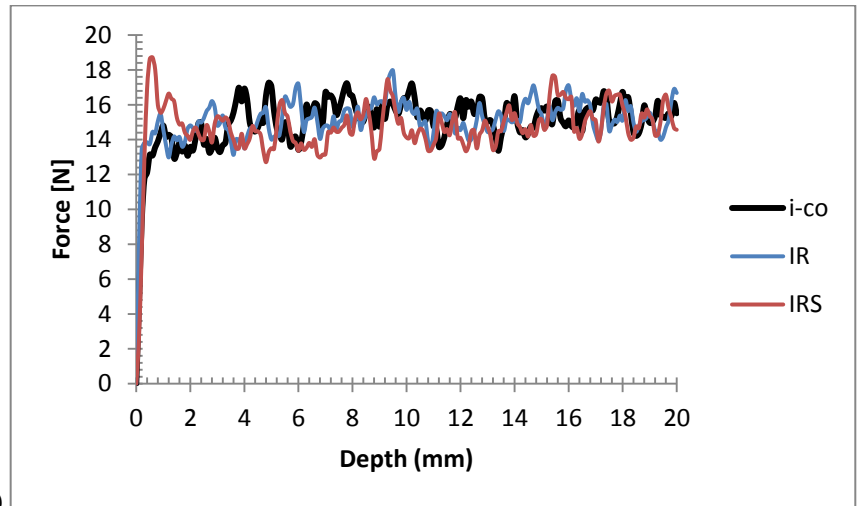
253 Drilling resistance results for the Indiana limestone samples are shown in Figure 4a and Table 5. The Indiana
 254 limestone shows a constant drilling resistance throughout the 20 mm drilling depth ($F \sim 15\text{N} (\pm 1.34)$). The samples
 255 treated with ET25 stored in room conditions showed no increase in the drilling resistance. In contrast, the samples
 256 treated with ET25 and sprayed with carbonated water (IRS), showed an increase in the drilling resistance ($F \sim 16.5$
 257 $\text{N} (\pm 1.43)$) within the outer 2-3 mm of the sample. These results are also in line with STT results that show that IRS
 258 samples present higher superficial cohesion after treatment. However, the increase in the drilling resistance in IRS
 259 sample is close to the experimental error.

260

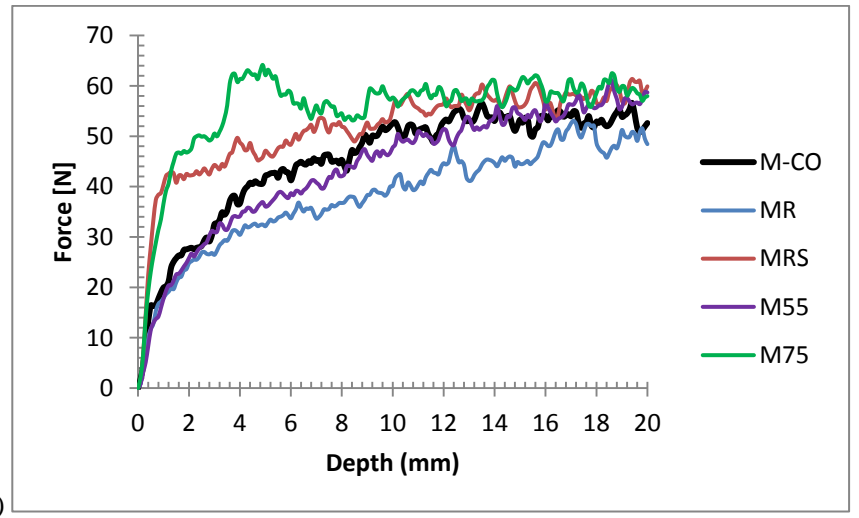
261 Drilling resistance results for the marble samples are shown in Figure 4b and Table 5. The drilling resistance of the
 262 weathered layer (up to 10-12 mm deep) is lower than in the core of the sample. The drilling resistance average in
 263 the outer 10 mm of the stone is $F \sim 37.4\text{N} (\pm 11.35)$, while for the inner 10 mm is $F \sim 53.5\text{N} (\pm 1.36)$. This result
 264 confirms that the formation of gypsum (CaSO_4) (see section 2.1) decreased the compactness of the stone on the
 265 surface. The treated marble samples which were sprayed with carbonated water (MRS) yielded a significant
 266 increase in the drilling resistance of the external weathered layer ($\Delta F \sim 51.82\%$) up to 10 mm. In contrast, samples

267 kept in the same room conditions (<50%RH) but not sprayed (MR) did not present any increase in the drilling
 268 resistance. This result clearly shows that a regular input of moisture enhances the carbonation of nanolime when in
 269 low relative humidity environments. Additionally, results also suggest that the inner values, due to the lower
 270 weathering of samples, are not affected by the treatment. MR and MR55 treated samples obtained lower drilling
 271 resistance compared to the control samples, probably due to the presence of a thicker layer of gypsum on their
 272 surface compared to the control samples. Marble samples which were treated and kept at 75%RH (M75) developed
 273 the highest increase in drilling resistance on the external weathered layer ($\Delta F \sim 72.12\%$). This confirms that a high
 274 relative humidity environment increases the nanolime effectiveness by providing a constant supply of moisture
 275 which enhances nanolime carbonation more than an intermittent input of moisture
 276

277



278



279 **Figure 4.** DRMS measurements of untreated (black line) and treated (colours) samples: a) Indiana limestone; b) marble
 280

Table 5. DRMS: experimental results

Force [N]	
Outer section (10mm)	Inner section (10 mm)

ICO	14.09 (± 0.89)	15.49 (± 0.62)
IR	14.4 (± 0.61)	15.41 (± 0.76)
IRS	16.06 (± 1.43)	15.51 (± 0.97)
M-CO	37.42 (± 11.35)	53.03 (± 1.62)
MR	30.20 (± 7.89)	49.15 (± 3.66)
MRS	45.84 (± 9.79)	57.38 (± 1.72)
M55	34.05 (± 9.40)	53.56 (± 1.83)
M75	51.98 (± 10.94)	58.76 (± 1.62)

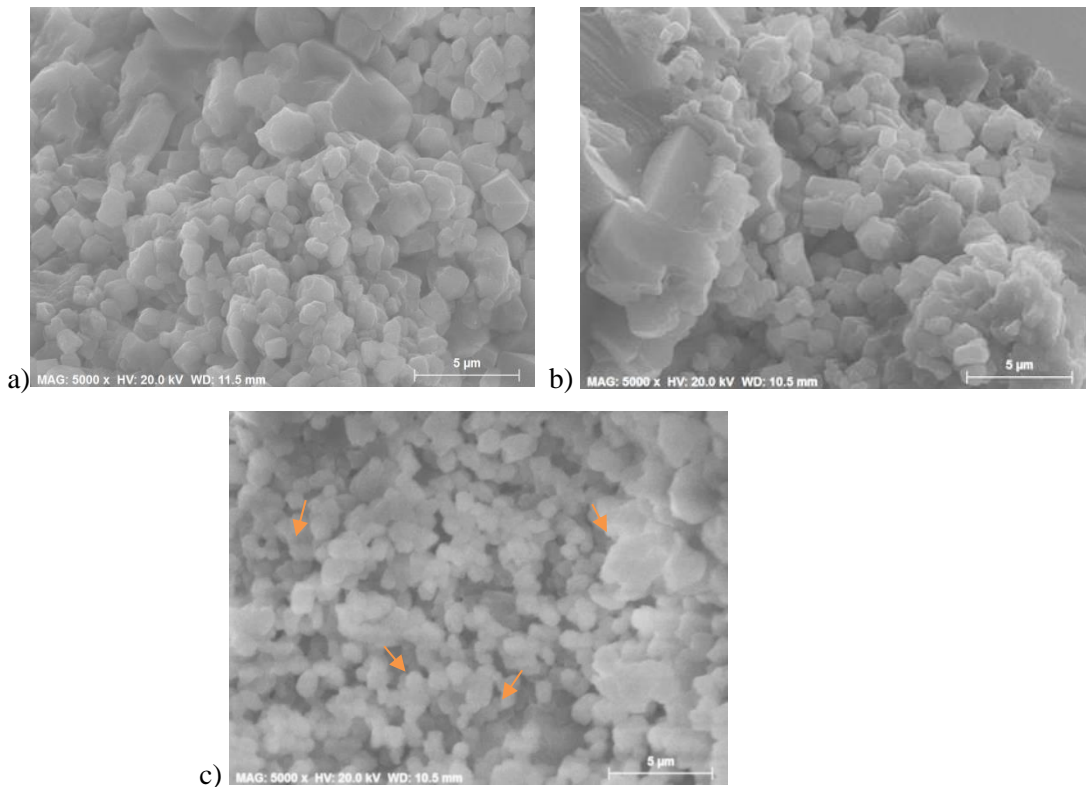
281

282

283 Cross-sections of treated surfaces were examined by SEM. In the case of the Indiana limestone, treated and
 284 untreated samples presented no significant differences in terms of morphology, as it is difficult to distinguish
 285 between the newly formed calcite crystals from nanolime and the calcite from the limestone. However, SEM
 286 images suggest that some newly formed calcite crystals from nanolime are present in the IRS samples, which seem
 287 to present smaller size compared to the calcite from the limestone (Figure 5c). This would be in line with DRMS
 288 and STT results, which show that these samples present higher drilling resistance in the surface which is attributed
 289 to the higher presence of carbonated nanolime particles.

290

291



292

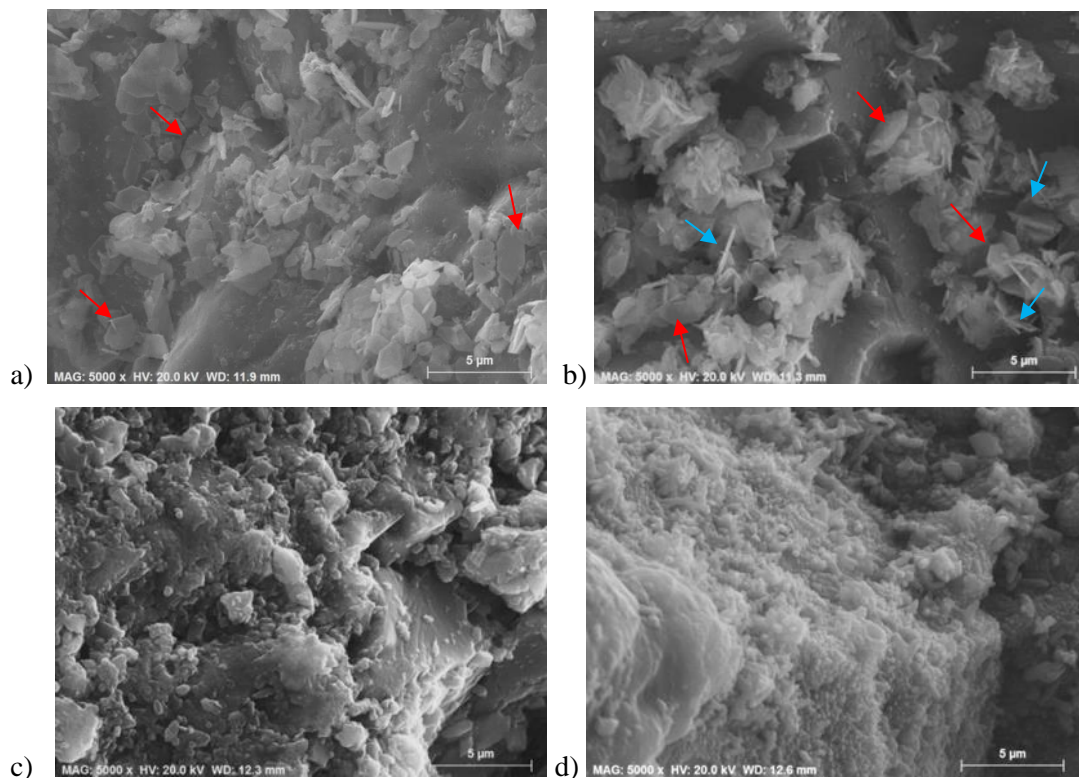
293 **Figure 5.** SEM images of Indiana Limestone samples all at 5,000X: a) I-CO; b) IR; c) IRS, where the orange arrows point to
 294 probable calcite crystals from the nanolime.

295

296 SEM images of marble samples show some hexagonal plates of portlandite crystals in the core of the samples
 297 which were kept at room conditions (MR) and at 55%RH (M55) (Fig. 6a and 6b). SEM images also suggest the
 298 possible presence of some gypsum crystals (Fig.6a and 6b). In contrast, no portlandite crystals were observed in
 299 samples which were sprayed with carbonated water (MRS) or kept at 75%RH (M75). Furthermore, both MRS and
 300 M75 seem to have higher amount of calcite crystals in the pores, which present smaller crystal size than the marble
 301 grains (Fig 6b and 6d). These results suggest that the increase in strength and the reduction in porosity of both
 302 samples (MRS and M75) could be attributed to a higher carbonation degree of the lime nano-particles. Recent
 303 research studies showed that the carbonation of nanoparticles synthesized by this method (anion exchange resins)
 304 dispersed in alcohol solvents can take more than a month to occur in low RH environments (<50%RH) and at high
 305 concentrations (i.e. 25 g/L) [45, 46].

306

307



308

309 **Figure 6.** SEM images of treated marble samples all at 5,000X where the red arrows point to Portlandite, and the blue ones to
 310 gypsum crystals: a) M-CO: b) MR , c) M55, d) MRS, e) M7.

311

312

313 The colorimetric analyses were carried out to evaluate the changes in L^* (white-black parameter) and ΔE^* (total
 314 colour variations) following treatment. Results (Table 6) show that all the treatments caused minor whitening of the
 315 stone surface with both ΔE^* and ΔL^* values above 5, apart from IR sample which resulted in both ΔE^* and ΔL^*

316 values <5. The whitening effect was slightly lower than that observed in the previous studies [14, 47]. This could
 317 be attributed to the fact that the application time in the previous tests was longer, resulting in an increased
 318 amount of nanolime deposition on the surface [14,47]. These values are slightly higher than the threshold
 319 recommended for consolidation treatments [48]. However, despite the increase in both ΔE^* and ΔL^* values, a
 320 recent study found that the whitening effect induced by consolidations with nanolime slightly decrease to values
 321 which are not perceivable by naked eye after moisture and UV light exposure without compromising its mechanical
 322 properties [24].

323

Table 6. Chromatic alterations for treated samples with regards to the control one.

	ΔL^*	Δa^*	Δb^*	ΔE^*
IR	6.61 (± 1.79)	-0.74 (± 0.04)	-0.19 (± 0.96)	6.65
IRS	4.43 (± 0.68)	-0.59 (± 0.13)	-0.63 (± 0.24)	4.51
MR	2.26 (± 0.43)	-0.05 ($\pm 0.0.19$)	-1.37 (± 3.46)	2.64
MRS	2.95 (± 3.31)	-0.46 (± 0.20)	1.81(± 0.42)	3.49
M55	1.18 (± 1.93)	-0.10 (± 0.34)	1.32 (± 0.66)	1.77
M75	2.34 (± 0.75)	-0.55 (± 0.12)	0.04 (± 2.19)	2.4

Mean Values determined on 30 measurements

324

325

326

327 **5 Conclusions**

328 This preliminary study has shown that nanolime can be used effectively for the consolidation of weathered marble
 329 stones with a gypsum surface layer. A solution of IP25 of nanolime synthesized by anion exchange processes is
 330 considered suitable for an in-situ application on the weathered marble sills of the west facade of the Reynolds
 331 Center, which houses both the Smithsonian’s National Portrait Gallery and the American Art Museum (Washington,
 332 D.C., USA). Nanolime may be applied during the wet season to increase the consolidation effectiveness, or, if
 333 applied during the dry season, marble surfaces should be sprayed regularly with carbonated water. In the case of the
 334 Indiana Limestone, which was not weathered, only a slight superficial consolidation was observed, although further
 335 research needs to be carried out on weathered samples.

336

337 In both stones the treatments that involved exposure to high relative humidity or spraying (IRS, MRS and M75)
 338 yielded a slightly higher consolidation effectiveness. Both treatments successfully recovered the surface cohesion
 339 of the stones as measured by Scotch Tape Test (STT). The treated samples which were sprayed with carbonated

340 water (IRS and MRS) obtained a higher increase in the surface cohesion compared to samples kept in the same
341 room conditions but without the addition of water by spraying. Marble samples kept at 75%RH obtained higher
342 consolidating results than those kept at 55%RH which confirms that higher moisture conditions enhance the
343 consolidation effectiveness. Drilling resistance results are in line with the STT results. Samples which were sprayed
344 with carbonated water (IRS and MRS) obtained a higher increase in the drilling resistance in both types of stone
345 than samples kept in the same environment without the input of moisture. IRS obtained a slight increase only in the
346 outer 2 mm of the sample, whereas the consolidation in MRS stones occurred throughout the sample but especially
347 in the outer 8 mm, where the weathered layer was consolidated. However, samples kept at 75%RH (M75) obtained
348 the highest increase in drilling resistance of the external weathered layer. This suggests that a high relative
349 humidity environment seems to increase the nanolime effectiveness by providing a constant supply of moisture
350 which enhances nanolime carbonation more effectively than an intermittent input of moisture such as that provided
351 by spraying. Conversely, samples stored at room conditions (50% RH) and samples kept at 55%RH obtained the
352 lowest drilling resistance due to a poorer carbonation rate. This could be associated with the reactivity of the
353 nanoparticles. Recent research showed that the carbonation of nanoparticles synthesized by anion exchange resins,
354 which are dispersed at high concentration (i.e. 25g/L) in pure alcohol solvents, can take more than a month to
355 carbonate in low RH environments [46].

356

357 Finally, these results suggest that for an on-site consolidation treatment with nanolime in dry environments, treated
358 surfaces should be regularly sprayed with carbonated water to increase its consolidation effectiveness.

359

360 **Acknowledgements**

361 This research has been funded by the Vice Chancellor's Scholarship within the Doctorate Program by Sheffield
362 Hallam University (UK) and through the Cantor Mobility Scholarship Scheme which funded my research stay at
363 the Smithsonian Institution (USA). Authors want to thank Dr. Anthony Bell (Sheffield Hallam University) for his
364 support with Rietveld refinements, Carol A. Grissom (Smithsonian's Museum Conservation Institute) for her help
365 in selecting the stones used for this testing and Dr. Thomas F. Lam (Smithsonian's Museum Conservation Institute)
366 for the SEM analysis.

367

368 **Conflict of interests**

369 The authors declare that there is no conflict of interest and take a neutral position to offer an objective evaluation of
370 the consolidation process.

371

372

373

374

375

376

377

378

379

380

381

382

383

384

385

386

387

388 **References**

389 [1] ICOMOS, (1964), "The Venice Charter", International Charter for the Conservation and Restoration of
390 Monuments and Sites.

391

- 392 [2] Doehne E., Price C. A., (2009), "Stone Conservation: An Overview of Current Research", Research in
393 conservation Series, Getty Conservation Institute, USA.
- 394
- 395 [3] Carta del Restauro, (1972), *Ideologie e prassi del restauro con Antologia di testi* G. La Monica, Libreria Nuova
396 Presenza, Palermo 1975, 213–230.
- 397
- 398 [4] Brandi, C., (1977), *Teoria del Restauro* Piccola Biblioteca Einaudi, Torino, 13–20.
- 399
- 400 [5] Wheeler G., (2008), "Alkoxysilanes and the consolidation of stone: Where we are now. In Stone Consolidation
401 in Cultural Heritage: Research and Practice", Proceedings of the International Symposium, Lisbon, 6-7 May 2008,
402 ed. J. Delgado-Rodriguez and J. M. Mimoso, 41-52. Lisbon: LNEC (Laboratorio Nacional de Engenharia Civil).
- 403
- 404 [6] Wheeler G., (2005), "Alkoxysilanes and Consolidation of stone", Research in conservation Series, Getty
405 Conservation Institute, USA.
- 406
- 407 [7] Ferreira-Pinto, A. P. and Delgado-Rodrigues J., (2008), "Hydroxylating conversion treatment and alkoxysilane
408 coupling agent as pre-treatment for the consolidation of limestones with ethyl silicate". In Stone Consolidation in
409 Cultural Heritage: Research and Practice; Proceedings of the International Symposium, Lisbon, 6-7 May 2008, ed.
410 J. Delgado-Rodriguez and J. M. Mimoso, 41-52. Lisbon: LNEC (Laboratorio Nacional de Engenharia Civil).
- 411
- 412 [8] Baglioni, P., Chelazzi D., Giorgi R., et al, (2014), "Commercial Ca(OH)₂ nanoparticles for the consolidation of
413 immovable works of art". Applied physics. A, Materials science & Processing, 114(3), pp.723–732
- 414
- 415 [9] Brajer I. and Kalsbeek N., (1999), "Limewater absorption and calcite crystal formation on a limewater-
416 impregnated secco wall-painting", Studies in Conservation vol. 44 (3), pp. 145–156.
- 417
- 418 [10] Price, C., Ross, K., White, G., (1988), "A further appraisal of the 'Lime Technique' for limestone
419 consolidation, using a radioactive tracer". IIC journal. Studies in Conservation, vol. 33 (4), pp.178–186.
- 420
- 421 [11] Otero J., Charola A. E., Grissom C. A., Starinieri V., (2017), "An overview of nanolime as a consolidation
422 method for calcareous substrates", Ge-conservacion, vol. 11, pp.71-78.
- 423 [12] Rodriguez-Navarro C., Ruiz-Agudo E., (2017), "Nanolimes: from synthesis to application", Pure and Applied
424 Chemistry, Volume 90, Issue 3, Pages 523–550, ISSN (Online) 1365-3075, ISSN (Print) 0033-4545,
425 DOI: <https://doi.org/10.1515/pac-2017-0506>.
- 426 [13] Ambrosi, M., Dei L., Giorgi R., et al., (2001), "Colloidal particles of Ca(OH)₂: Properties and applications to
427 restoration of frescoes", Langmuir, 17(14), pp.4251–4255.
- 428

- 429 [14] Samanta, A., Chanda D. K., Das P. S., et al., (2016), "Synthesis of nano calcium hydroxide in aqueous
430 medium". *Journal American Ceramic Society*, 795(37004), pp.787–795.
- 431
- 432 [15] Nanni, A., Dei, L., (2003), "Ca(OH)₂ nanoparticles from W/O microemulsions". *Langmuir*, 19(13), pp.933–
433 938.
- 434
- 435 [16] Sequeira, S., Casanova C., Cabrita E. J., (2006), "Deacidification of paper using dispersions of Ca(OH)₂
436 nanoparticles in isopropanol", *Journal Cultural Heritage*, 7, pp.264–272.
- 437
- 438 [17] Daniele, V. and Taglieri, G., (2012), "Synthesis of Ca(OH)₂ nanoparticles with the addition of Triton X-100.
439 Protective treatments on natural stones: Preliminary results". *Journal of Cultural Heritage*, 13(1), pp.40–46.
- 440
- 441 [18] Poggi, G., Toccafondi N., Chelazzi D., et al, (2016), "Calcium hydroxide nanoparticles from solvothermal
442 reaction for the deacidification of degraded waterlogged wood". *Journal of Colloid and Interface Science*, 473,
443 pp.1–8.
- 444
- 445 [19] Borsoi, G., Lubelli B., Van Hees R. et al., (2016), "Effect of solvent on nanolime transport within limestone:
446 How to improve in-depth deposition". *Colloids and Surfaces A: Physicochemical and Engineering Aspects*, 497,
447 pp.171–181.
- 448
- 449 [20] Liu, T., Zhu Y., Zhang X., et al., (2010), "Synthesis and characterization of calcium hydroxide nanoparticles
450 by hydrogen plasma-metal reaction method". *Materials Letters*, 64(23), pp.2575–2577.
- 451
- 452 [21] Volpe R., Taglieri G., Daniele V., et. al., (2016), "A process for the synthesis of Ca(OH)₂ nanoparticles by
453 means of ionic exchange resin", European patent EP2880101
- 454
- 455 [22] Taglieri, G., Daniele V. Del Re, et al, (2015), "A new and original method to produce Ca(OH)₂ nanoparticles
456 by using an anion exchange resin". *Advances in Nanoparticles*, 4, pp.17–24.
- 457
- 458 [23] Taglieri G., Otero J., Daniele V., et. al., (2017), "The biocalcarenite stone of Agrigento (Italy): Preliminary
459 investigations of compatible nanolime treatments", *Journal of Cultural Heritage*,
460 <https://doi.org/10.1016/j.culher.2017.11.003>.
- 461
- 462 [24] Otero J., Starinieri V., Charola A. E., (2018), "Nanolime for the consolidation of lime mortars: a comparison
463 of three available products", *Journal of Construction and Building Materials* Vol. 181, pp.394-407.
- 464
- 465 [25] Otero J., Starinieri V., Charola A. E., (2019), "Influence of substrate pore structure and nanolime particle size
466 on the effectiveness of nanolime treatments", *Journal of Construction and Building Materials* (in-press).

- 467 [26] Daniele V., Taglieri G., Macera L., et al, (2018), "Green approach for an eco-compatible consolidation of the
468 Agrigento biocalcarenite surface", *Journal of Construction and Building Materials*, vol. 186, pp.1188-1199.
- 469 [27] Giorgi R., Dei L., Ceccato M., et al, (2002), "Nanotechnologies for Conservation of Cultural Heritage: Paper
470 and Canvas Deacidification", *Langmuir* 18(21), pp.8198-8203. **DOI:** 10.1021/la025964d
471
- 472 [28] Natali I., Tempesti P., Carretti E., et al, (2014), "Aragonite Crystals Grown on Bones by Reaction of CO₂ with
473 Nanostructured Ca(OH)₂ in the Presence of Collagen. Implications in Archaeology and Paleontology", *Langmuir*
474 30(2), 660-668.
475
- 476 [29] Pondelak, A., Kramar, S., Lesar Kikelj, M., Sever Skapin, A., (2017), "In-situ study of the consolidation of
477 wall paintings using commercial and newly developed consolidants", *Journal of Cultural Heritage*, 28, pp. 1-8
478
- 479 [30] Taglieri, G., Daniele, V., Macera, L., Mignemi A., "Innovative and green nanolime treatment tailored to
480 consolidate the original mortar of the façade of a medieval building in L'Aquila (Italy)", (2019) *Construction and*
481 *Building Materials* 221, pp. 643-650
482
- 483 [31] Tzavellos, S., Pesce, G.L., Wu, Y., Henry, A., Robson, S., Ball, R.J., (2019), "Effectiveness of Nanolime as a
484 Stone Consolidant: A 4-Year Study of Six Common UK Limestones", *Materials*, 12, 2673
485
- 486 [32] Gherardi F., Otero J., Blakeley R., Colston B., (2020), "Application of Nanolimes for the Consolidation of
487 Limestone from the Medieval Bishop's Palace, Lincoln, UK", *Studies in Conservation*, DOI:
488 10.1080/00393630.2020.1752436
489
- 490 [33] Rossi Manaresi R., Charola A. E., Tucci A., et al., (1984), "Study of accelerated weathering of limestones
491 treated with an acrylic-silicone mixture", *ICOM 7th Triennial Meeting, Copenhagen*. pp. 84.10.1-84.10.4. Paris:
492 ICOM-J. Paul Getty Trust.
493
- 494 [34] Folk R. L., (1959), "ractical petrographic classification of limestone", *Am. Assoc. Pet. Geol. Bull.* 43 (1) 1–38.
495
- 496 [35] Dunham R. J., (1962), "Classification of carbonate rocks according to depositional texture. In Ham, W.E.
497 classification of carbonate rocks", *Am. Assoc. Petroleum Geologists Mem.* 1,108–121
498
- 499 [36] Rietveld H.M., (1969), "A profile refinement method for nuclear and magnetic structures", *Journal Applied*
500 *Crystallography*, 10, 65.
501

- 502 [37] Bish D. L. and Post J. E., (1989), Modern powder diffraction. Mineralogical Society of America, Crystal
503 Reasearch & Technology, Washington. ISBN 0 - 939950 - 24 - 3.
504
- 505 [38] Charola A. E. and Ware R., (2002), "Acid deposition and the deterioration of stone: a brief review of a broad
506 topic", Geological society, London, Special Publication, 205, 393-406.
507 DOI: <https://doi.org/10.1144/GSL.SP.2002.205.01.28>
508
- 509 [39] Daniele, V., Taglieri, G., (2010), "Nanolime suspensions applied on natural lithotypes: The influence of
510 concentration and residual water content on carbonatation process and on treatment effectiveness". Journal of
511 Cultural Heritage, 11(1), pp.102–106.
512
- 513 [40] Rodriguez-Navarro, C., Bettori I, Ruiz-Agudo E., (2016), "Kinetics and mechanism of calcium hydroxide
514 conversion into calcium alkoxides: Implications in heritage conservation using nanolimes", Langmuir, 32(20), pp.
515 5183-5194.
516
- 517 [41] ASTM C 67-00: Standard Test Methods for Measuring Apparent Porosity at atmospheric pressure, (2000),
518 ASTM
519
- 520 [42] ASTM D3359-02: Standard Test Methods for Measuring Adhesion by Tape Test, (2002), ASTM International,
521 10 August.
522
- 523 [43] Costa D., Delgado-Rodrigues J., (2012), "Consolidation of a porous limestone with nano-lime", in: G. Wheeler
524 (Ed.), 12th International congress on the deterioration and conservation of stone, New York, pp. 10–19.
525
- 526 [44] Rodriguez-Navarro C., Suzuki A., Ruiz-Agudo E., (2013), "Alcohol dispersions of calcium hydroxide
527 nanoparticles for stone conservation", Langmuir vol. 29, pp. 11457–11470.
528
- 529 [45] López-Arce, P., Gomez-Villalba L.S., Pinho L., et al., (2010), "Influence of porosity and relative humidity on
530 consolidation of dolostone with calcium hydroxide nanoparticles: Effectiveness assessment with non-destructive
531 techniques". Materials Characterization, 61(2), pp.168–184.
532
- 533 [46] Taglieri G, Daniele V., Macera L., Mondelli C., (2017), "Nano Ca(OH)₂ synthesis using a cost-effective and
534 innovative method: Reactivity study", J Am Ceram Soc. 2017;100:5766–5778
- 535 [47] Pozo-Antonio J.S., Otero J., Alonso P., et al., (2019), "Nanolime and Nanosilica applied on heated granite and
536 limestone: effectiveness and durability", Journal of Construction and Building Materials (in-press).
537

538 [48] R. F. Witzel, R. W. Burnham, and J. W. Onley. Threshold and suprathreshold perceptual color differences. J.
539 Optical Society of America, 63:615, 1973
540
541
542
543
544